

Article

Time-Varying Wind-Resistance Global Reliability Analysis of In-Service Transmission Tower Using High-Order Moments-Based Improved Maximum Entropy Method

Cheng Liu ¹, Tao Wang ^{2,3,*} , Zhengqi Tang ¹ and Zhengliang Li ^{1,4}¹ School of Civil Engineering, Chongqing University, Chongqing 400045, China² School of Transportation Science and Engineering, Harbin Institute of Technology, Harbin 150040, China³ Chongqing Research Institute of Harbin Institute of Technology, Harbin Institute of Technology, Chongqing 401151, China⁴ Key Laboratory of New Technology for Construction of Cities in Mountain Area (Chongqing University), Ministry of Education, Chongqing 400045, China

* Correspondence: taowang@cqu.edu.cn; Tel.: +86-15123044500

Abstract: The transmission tower is an important infrastructure for transmission lines. To secure the operation of the power grid, it is particularly important to evaluate the safety of the in-service transmission tower under the action of random wind loads throughout their entire life cycle. Thus, this paper firstly establishes the time-varying equivalent performance function of the in-service transmission tower under the action of random wind loads. Then, in order to address the shortcomings of the traditional maximum entropy method, the high-order moments-based improved maximum entropy method (HM-IMEM) is proposed and extended to assess the wind resistance global reliability of the in-service transmission tower. Finally, the effectiveness of the proposed method is demonstrated evaluating the wind resistance global reliability of an in-service transmission tower in an engineering setting. Analytic results indicate that: (1) The proposed method can ensure a balance between calculation accuracy and efficiency. Compared with Monte Carlo simulation (MCS) method, the relative error is only 0.11% and the computational cost is much lower than that of the MCS method. (2) The reliability of the in-service transmission tower significantly decreased over time. In order to guide maintenance and reinforcement by predicting the time-varying performance of in-service transmission towers, it is of great engineering value to evaluate the wind resistance global reliability of the in-service transmission tower.

Keywords: in-service transmission tower; wind resistance global reliability; time-varying system; HM-IMEM; time-varying equivalent performance function



Citation: Liu, C.; Wang, T.; Tang, Z.; Li, Z. Time-Varying Wind-Resistance Global Reliability Analysis of In-Service Transmission Tower Using High-Order Moments-Based Improved Maximum Entropy Method. *Appl. Sci.* **2023**, *13*, 4245. <https://doi.org/10.3390/app13074245>

Academic Editor: Angelo Luongo

Received: 6 March 2023

Revised: 25 March 2023

Accepted: 26 March 2023

Published: 27 March 2023



Copyright: © 2023 by the authors. Licensee MDPI, Basel, Switzerland. This article is an open access article distributed under the terms and conditions of the Creative Commons Attribution (CC BY) license (<https://creativecommons.org/licenses/by/4.0/>).

1. Introduction

In recent years, ultra-high voltage (UHV) transmission lines were rapidly developed in China. Transmission towers are important infrastructure for transmission lines and their safety is directly related to the operation of the line [1–3]. Due to prolonged exposure to the atmosphere, the steel members of transmission towers are prone to rust and corrosion under the effect of acid rain, leading to the degradation of tower performance. In this regard, it is of great engineering significance to conduct global time-varying reliability analysis of transmission towers to predict the service performance.

The current global reliability analysis methods for transmission towers mainly include the Monte Carlo simulation (MCS) method [4], failure mode identification method [5–7], and performance function equivalent description method [8]. Although the MCS method is simple and easy to implement, it is not suitable for global reliability analysis of large and complex transmission towers due to its high computational cost. Refs. [6,7] combined the failure mode identification method with the Ditlevsen bounds method for the global

reliability analysis of transmission towers. However, it is difficult to identify the failure mode due to the large number of members in transmission towers, and the correlation between any two failure modes was not reasonably considered. It is worth pointing out that the Ref. [9] studied the global reliability of transmission towers by combining the equivalent description method of the performance function and high-order moment method. The equivalent description of the performance function reasonably considers the correlations of these failure modes. Nevertheless, existing research on the reliability of transmission towers still focuses on time-invariant global reliability analysis, and research on time-varying global reliability of in-service transmission towers in relation to performance degradation is rarely reported.

Compared to research on time-invariant global reliability, research on time-varying global reliability is more challenging and computationally expensive. Over the past few decades, research on time-varying reliability received great attention and some novel methods were proposed, e.g., the time-discrete-integrated method [10], first transcendental reliability conversion method [11–13], time-invariant and time-varying reliability conversion method [14], probability density evolution method [15], and MCS [16]. However, these relevant studies mostly limit time-varying reliability analysis to the member level. Ref. [17] proposed a time-varying global reliability analysis method based on high-order moments, and the results indicate that this method can provide good precision for simple structural systems. However, the order of the required high-order moments is determined subjectively in this method, and the introduction of the dimension reduction method (DRM) cannot guarantee the required accuracy for complex engineering structures. In general, there is a lack of research on methods to analyze time-varying global reliability that can achieve a better tradeoff between accuracy, efficiency, and versatility for in-service transmission towers.

The objective of this paper is to develop a time-varying global reliability analysis method for in-service transmission towers that can effectively evaluate their time-varying global reliability with a tradeoff between accuracy and efficiency. The remainder of this paper is organized as follows: In Section 2, the time-varying equivalent performance function for in-service transmission towers under the action of random wind loads is established. In Section 3, the high-order moments-based improved maximum entropy method (HM-IMEM) is proposed, and the time-varying global reliability analysis for in-service transmission towers is presented based on the HM-IMEM. In Section 4, focusing on an in-service transmission tower in practice, the analysis of time-varying global reliability under the action of random wind loads is investigated using HM-IMEM. Finally, some conclusions are summarized in Section 5.

2. The Time-Varying Performance Function of In-Service Transmission Towers

2.1. Resistance Degradation Model for Steel Members

The resistance of in-service transmission towers in corrosive atmospheric environments degrades over time. As transmission towers are primarily composed of circular steel tubes or angle steel, the resistance degradation model of steel members must be examined first in order to describe their time-varying performance. However, most studies on resistance degradation models focus on reinforced concrete, with relatively few studies centering around steel members [18,19]. In this paper, the degradation process of steel members is described based on the idea of the attenuation function method [20,21]. The initial value is R_0 , and the resistance $R(t)$ at any time can be expressed by the following equation:

$$R(t) = R_0\zeta(t) \quad (1)$$

where R_0 is usually considered a random variable, and $\zeta(t)$ is the function that describes resistance degradation over time.

2.2. Random Equivalent Static Wind Loads of Transmission Towers

The dynamic reliability analysis of transmission towers under wind loads is complicated, and the corresponding theory is not yet fully developed. One of the frequently used methods is to simplify dynamic wind loads into equivalent static wind loads, and then convert dynamic reliability into static reliability. According to Ref. [9], the mean, standard deviation, and probability distribution of random equivalent static wind loads can be expressed as follows:

$$\mu_{W_{se}} = \mu_{\beta_z} \mu_{W_s} \tag{2a}$$

$$\sigma_{W_{se}} = \sqrt{\mu_{W_s}^2 \sigma_{\beta_z}^2 + \beta_z^2 \sigma_{W_s}^2} \tag{2b}$$

$$F_{W_{se}}(w) = \exp \left\{ - \exp \left[- \frac{w - [1 - 0.45\delta_{W_{se}}] \mu_{W_{se}}}{0.779\delta_{W_{se}} \cdot \mu_{W_{se}}} \right] \right\} \tag{2c}$$

where $\delta_{W_{se}}$ is the coefficient of variation in the random equivalent static wind loads W_{se} , μ_{W_s} and σ_{W_s} are mean and standard deviation of the random static wind loads W_s , and μ_{β_z} and σ_{β_z} are mean and standard deviation of the random wind vibration coefficient β_z .

Since wind loads are taken as the maximum value during the design reference period [10], the probability distribution of the maximum random equivalent static wind loads during the design reference period T can be further expressed as

$$F_{W_{seT}}(w) = \exp \left\{ - \exp \left[- \frac{w - [1 - (0.45 - 0.779 \ln T)\delta_{W_{se}}] \mu_{W_{se}}}{0.779\delta_{W_{se}} \cdot \mu_{W_{se}}} \right] \right\} \tag{3}$$

and the corresponding mean and standard deviation can be calculated as follows:

$$\begin{cases} \mu_{W_{seT}} = (1 + 0.779\delta_{W_{se}} \ln T) \mu_{W_{se}} \\ \sigma_{W_{seT}} = \sigma_{W_{se}} \end{cases} \tag{4}$$

2.3. The Equivalent Description of the Time-Varying Performance Function of In-Service Transmission Towers

The main member is the primary bearing member of the transmission tower system, and it plays a crucial role in the structural design of the tower [9]. Therefore, using the failure criterion that the stress of the main member exceeds the yield strength, the equivalent performance function of in-service transmission towers can be established based on the equivalent description method [22] and the resistance degradation model shown in Equation (1). This function can be expressed as

$$Z(t) = \min_{i=1,2,\dots,l} [R(t) - S_i(W_{seT}, t)] \tag{5a}$$

$$\begin{cases} S_i(W_{seT}, t) = \frac{N_c(t)}{\varphi A} + \frac{M(t)}{\omega} \text{ for compression - bending member} \\ S_i(W_{seT}, t) = \frac{N_t(t)}{A} + \frac{M(t)}{\omega} \text{ for tension - bending member} \end{cases} \tag{5b}$$

in which $Z(t)$ denotes the time-varying equivalent extreme variable, $R(t)$ denotes the time-varying yield strength of the main member, and l is the number of main members. $S_i(W_{seT}, t)$ denotes the time-varying stress of each main member under random equivalent static wind loads, $N_c(t)$ is the time-varying axial compression force, $N_t(t)$ is the time-varying axial tension force, $M(t)$ is the time-varying bending moment, φ is the stability coefficient under axial compression, A is the area of cross-section, and ω is the cross-section modulus [23].

3. The Time-Varying Global Reliability Analysis Based on the HM-IMEM

3.1. The Traditional Maximum Entropy Method Based on the First four Moments

The traditional maximum entropy method (MEM) uses the first four raw moments $M_{Z,k}$ ($k = 0, 1, \dots, 4$) of the performance function Z as constraint conditions and the Shannon

entropy H_s of the Z as the objective function. The following optimization model can be established as [24]:

$$\begin{aligned} \max H_s &= \int_{-\infty}^{\infty} f_Z(z) \ln f_Z(z) dz \\ \text{s.t.} \quad &\begin{cases} \int_{-\infty}^{\infty} z^k f_Z(z) dz = M_{Z,k}, k = 1, 2, 3, 4 \\ \int_{-\infty}^{\infty} f_Z(z) dz = 1 \end{cases} \end{aligned} \tag{6}$$

Based on the penalty function method [25,26], Equation (6) can be converted to the unconstrained optimization problem, namely:

$$L = -H_s + \lambda_0 \left(\int_{-\infty}^{\infty} f_Z(z) dz - 1 \right) + \sum_{k=1}^n \lambda_k \left[\int_{-\infty}^{\infty} z^k f_Z(z) dz - M_{Z,k} \right] \tag{7}$$

By solving the unconstrained optimization problem shown in Equation (7) with the help of the Newton method or quasi-Newton method [27–29], coefficients $\lambda_0, \lambda_1, \dots,$ and λ_4 can be obtained. Then, the maximum entropy probability density function (PDF) $f_Z(z)$ and the failure probability P_f of the Z can be calculated as follows, respectively:

$$f_Z(z) = \exp \left(\lambda_0 - \sum_{k=1}^4 \lambda_k z^k \right) \tag{8a}$$

$$P_f = P(Z \leq 0) = \int_{-\infty}^0 \exp \left(\lambda_0 - \sum_{k=1}^4 \lambda_k z^k \right) dz. \tag{8b}$$

Although the traditional MEM is widely used in reliability analysis, there are still some issues with its accuracy and convergence. This is because the traditional MEM usually uses the dimension reduction method (DRM) for statistical moment estimation and only considers the first four moments as constraints [24]. This may lead to poor precision of the reliability index if the first four moments are not accurate enough or if the probability information is incomplete [30]. In addition, the traditional MEM usually determines the maximum entropy integral limits subjectively, which can result in numerical instability or even divergence of the MEM [31].

In this regard, the generalized F-discrepancy (GF-discrepancy)-based point selection method [32], which can effectively control the estimation error, is introduced to estimate high-order statistical moments of the performance function based on Equations (6)–(8b). Meanwhile, the integral limits determination method and convergence criterion are introduced to rationally determine the integral limits and the order of the required high-order moments of the MEM, respectively. Furthermore, a new maximum entropy method is proposed noted as the high-order moments-based improved maximum entropy method (HM-IMEM). Finally, the HM-IMEM is applied to analyze the time-varying global reliability of the in-service transmission tower.

3.2. The High-Order Moments-Based Improved Maximum Entropy Method

3.2.1. The Estimation of the High-Order Moments Based on the GF-Discrepancy-Based Point Selection Method

Recently, there was a growing interest in the GF-discrepancy-based point selection method [32] due to its balanced distribution of point sets and effective control of error limits. Therefore, to address the issue of inadequate accuracy of high-order moments in the dimension reduction integral method for complex systems, the GF-discrepancy-based point selection method is introduced in this paper.

Firstly, a brief description of the theory and implementation of the GF-discrepancy-based point selection method is provided. Supposing the representative point set corre-

sponding to the random vector X is noted as $\{x_q, q = 1, 2, \dots, N_T\}$, and the GF-discrepancy D_{GF} corresponding to the representative point set can be defined as

$$D_{GF} = \max_{1 \leq i \leq n} \{ \sup |E_i(x) - F_i(x)| \} \tag{9}$$

in which $F_i(x)$ is the marginal cumulative probability distribution function of X_i and $E_i(x)$ is the empirical cumulative probability distribution function of X_i , namely

$$E_i(x) = \sum_{q=1}^{N_T} w_q \cdot I(x_{q,i} \leq x) \tag{10}$$

$$w_q = \int_{\Omega_q} \rho_X(x) dx \tag{11}$$

where $I(\cdot)$ is the indication function, and w_q is the weight coefficient and also called the probability of assignment, which can be estimated by the probability measure in a set of representative regions. For a given representative point set, its representative regions can be adopted by Voronoi cell-based partition technique [33].

In this paper, using the procedure of GF-discrepancy-based point selection method shown in Equations (9)–(11), the Sobol sequence [34] is employed to generate n -dimensional independent point set $I_n = \{u_q = (u_{q,1}, u_{q,2}, \dots, u_{q,n}), q = 1, 2, \dots, N_T\}$, which is uniformly distributed in $[0, 1]^n$. The initial point set $x_{q,I}$ corresponding to X can be generated as follows:

$$x_{q,i} = F_i^{-1}(u_{q,i}), i = 1, \dots, n, q = 1, \dots, N_T \tag{12}$$

where $F_i^{-1}(\cdot)$ is the inverse function of $F_i(\cdot)$.

To minimize the GF-discrepancy of the selected point set, $\theta_{q,i}$ shown in Equation (12) is reconstructed twice as follows:

$$x'_{q,i} = F_i^{-1} \left(\sum_{k=1}^{N_T} \left(\frac{I(x_{k,i} \leq x_{q,i})}{N_T} \right) + \frac{1}{2} \cdot \frac{1}{N_T} \right) \tag{13a}$$

$$x''_{q,i} = F_i^{-1} \left(\sum_{k=1}^{N_T} (w_k \cdot I(x'_{k,i} \leq x'_{q,i})) + \frac{1}{2} w_q \right) \tag{13b}$$

where $x'_{q,i}$ and $x''_{q,i}$ denote the reconstructed point sets.

The point set $x''_{q,i}$ and weight coefficient w_q obtained by GF-discrepancy-based point selection method are used to calculate raw moments $M_{z,k}$ of the performance function, namely.

$$M_{Z,k} = E(Z^k) = \sum_{q=1}^{N_T} w_q (Z(x''_q))^k \tag{14}$$

3.2.2. The Determination of Integral Limits

It is easy to find that the integrals shown in Equations (6) and (7) are defined over the infinite domain $(-\infty, +\infty)$ where the integrals are difficult to be calculated directly. In practice, the infinite domain is frequently replaced by the finite domain $(\mu - 10\sigma, \mu + 10\sigma)$, where μ and σ are the mean and standard deviation of the performance function, respectively. However, the convergence of the integral problem greatly depends on the accuracy of the integral limits. Obviously, the approximation on the finite domain $(\mu - 10\sigma, \mu + 10\sigma)$ is subjective and may lead to truncation errors, and even make the MEM not converge. In this regard, to enhance the numerical stability and accuracy, a more

rational determination of the integral limits is introduced in this section [31]. Firstly, the linearly shifter moment m_i involving an unknown variable C can be defined [35] as follows:

$$m_i = \sum_{j=0}^i \binom{i}{j} (-C)^{i-j} M_{Z,j} \tag{15}$$

and then, the following equations containing variable C can be constructed, namely

$$\tau = \Delta_1 / \Delta_2 \tag{16a}$$

in which

$$\Delta_1 = \det \begin{bmatrix} m_0 & m_1 & \cdots & m_{n'} \\ m_1 & m_2 & \cdots & m_{n'+1} \\ \vdots & \vdots & \ddots & \vdots \\ m_{n'} & m_{n'+1} & \cdots & m_{2n'} \end{bmatrix} \tag{16b}$$

$$\Delta_2 = \det \begin{bmatrix} m_0 & m_1 & \cdots & m_{n'+1} \\ m_1 & m_2 & \cdots & m_{n'+2} \\ \vdots & \vdots & \ddots & \vdots \\ m_{n'+1} & m_{n'+2} & \cdots & m_{2n'+2} \end{bmatrix}. \tag{16c}$$

The solutions about the variable C , noted as ζ' and ζ , can be obtained by solving the Equation (16a), where n' equals to $\lfloor n/2 \rfloor$ and τ equals to $10^{-(n'+1)}$. Finally, ζ' and ζ are considered as the upper and lower integral limits, respectively.

3.2.3. Convergence Mechanism

Theoretically, as the order of moments in the constrained condition of Equation (6) increases, the probability density function (PDF) fitted by the MEM approaches the true value more closely. However, estimating high-order moments often requires significant computational resources to achieve the satisfactory accuracy. Therefore, it is important to keep a balance between accuracy and efficiency. To this end, the convergence mechanism in Ref. [30] is introduced to automatically determine the order of moments, namely

$$\frac{\|H_s - H_{s-2}\|}{\|H_s\|} \leq \varepsilon \tag{17}$$

where ε is a specific positive error precision value and is taken as 10^{-5} here.

If Equation (17) is satisfied, the Shannon entropy H_s converges to a stable value. That is, the first s -order raw moments can accurately reconstruct the maximum entropy PDF.

3.2.4. The Structural Reliability Analysis

Using Equation (7) and combing the first s -order raw moments $M_{z,k}$ obtained from Equation (14) with the integral limits ζ' and ζ calculated by Equation (16a), the objective function of the unconstrained optimization problem can be expressed as follows:

$$L = -H_s + \lambda_0 \left(\int_{\zeta}^{\zeta'} f_Z(z) dz - 1 \right) + \sum_{k=1}^n \lambda_k \left[\int_{\zeta}^{\zeta'} z^k f_Z(z) dz - M_{Z,k} \right]. \tag{18}$$

Similarly, the maximum entropy PDF $f_Z(z)$ can be estimated by the Newton method as

$$f_Z(z) = \exp \left(\lambda_0 - \sum_{k=1}^s \lambda_k z^k \right). \tag{19}$$

Then, based on the maximum entropy PDF of Equation (19) and the lower integral bound ζ , the structural failure probability and reliability index can be calculated, namely

$$\begin{cases} P_f = P_f(Z \leq 0) = \int_{\zeta}^0 \exp\left(\lambda_0 - \sum_{q=1}^s \lambda_q z^q\right) dz \\ \beta = -\Phi^{-1}(P_f) \end{cases} \quad (20)$$

in which $\Phi^{-1}(\cdot)$ denotes the inverse function of the cumulative distribution function of standard normal variable $\Phi(\cdot)$.

3.3. Numerical Implementation of the HM-IMEM for Time-Varying Global Reliability of In-Service Transmission Towers

By combining the established time-varying equivalent performance function of in-service transmission towers with the proposed HM-IMEM, the time-varying global reliability analysis of in-service transmission towers under action of random wind loads can be carried out in the following implementation steps (see also the flowchart in Figure 1):

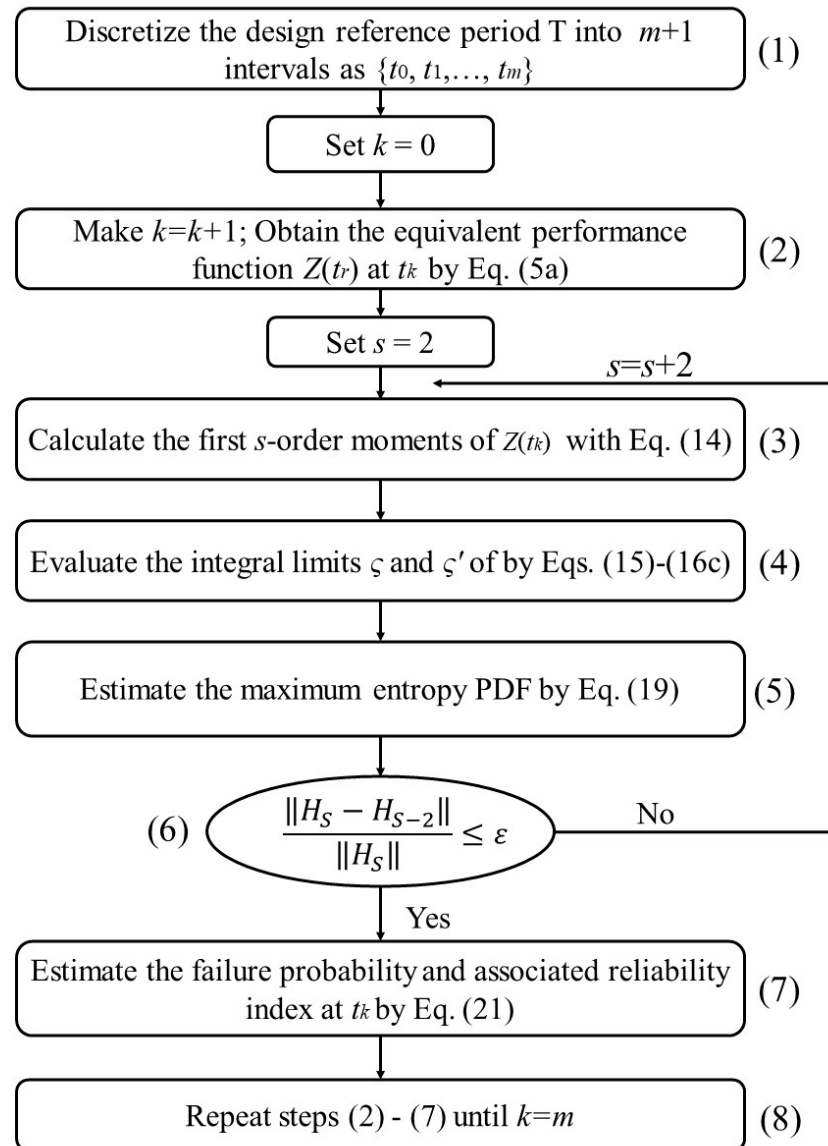


Figure 1. A flowchart to illustrate the implementation procedure of the proposed method.

Step1: Discretization of the design reference period.

The design reference period $T = [t_0, t_m]$ is equally divided into $m + 1$ intervals, each interval is $\Delta t = (t_m - t_0)/m$ in length, and the design reference period T can be discretized into $\{t_0, t_1 = t_0 + \Delta t, \dots, t_m = t_0 + m \cdot \Delta t\}$ intervals.

Step2: The equivalent description of the time-varying performance function.

According to Equation (5a), the equivalent performance function $Z(t_r)$ of the in-service transmission tower at $t_r = t_0$ can be obtained.

Step3: The statistical moments estimation for $Z(t_r)$.

Based on Equation (14) and taking $s = 2$, the first s -order moments of the $Z(t_r)$ are calculated at $t_r = t_0$.

Step4: Calculation of integral limits.

Based on Equations (15) and (16c), the integral limits ζ and ζ' of the HM-IMEM can be obtained.

Step5: Calculation of the maximum entropy PDF.

With the first s -order moments, the maximum entropy PDF can be estimated by Equation (19).

Step6: Convergence mechanism.

If the Equation (17) is satisfied, the next step will be implemented; otherwise, go back to step (3) and make $s = s + 2$.

Step7: Estimation of the failure probability and reliability index for the in-service transmission tower at t_r .

The failure probability and reliability index of the in-service transmission tower at t_r can be calculated according to Equation (20), but with a time parameter, namely

$$\begin{cases} P_f(t_r) = \int_{\zeta(t_r)}^0 \exp\left(\lambda_0(t_r) - \sum_{q=1}^{s(t_r)} \lambda_q(t_r) z^q(t_r)\right) dz \\ \beta(t_r) = -\Phi^{-1}(P_f(t_r)) \end{cases} \quad (21)$$

Step8: Calculation of the time-varying failure probability and reliability index of the in-service transmission tower.

Repeating steps (2)–(7), and calculating the failure probability, $\{P_f(t_1), P_f(t_2), \dots, P_f(t_m)\}$, and the reliability index, $\{\beta(t_1), \beta(t_2), \dots, \beta(t_m)\}$ at $r = 1, 2, \dots, m$, respectively.

4. Example Analysis

4.1. Engineering Situation and the Finite Element Model of the In-Service Transmission Tower

In this paper, an in-service UHV tower on the Jindongnan-Nanyang-Jingmen line in China is used as the engineering background [36]. The Jindongnan-Nanyang-Jingmen transmission line project is the initial project for the development of UHV transmission in China, and it is necessary to analyze the time-varying wind resistance global reliability of in-service transmission towers on the Jindongnan-Nanyang-Jingmen line. A typical in-service transmission tower on this transmission line is selected for time-varying wind resistance global reliability analysis. This in-service transmission tower has a height of 181.8 m, a square plane shape, and is built with lattice steel tubes made of Q345 steel and Q235 steel. In this paper, the general FEA software ANSYS was applied for the structural analysis of the transmission tower, which was analyzed by depending on the ideal elastic-plastic constitution of steel. Meanwhile, the transmission tower was composed by steel tubes, which were simulated by Beam 188 element in ANSYS, and the FE model of the in-service transmission tower is shown in Figure 2.

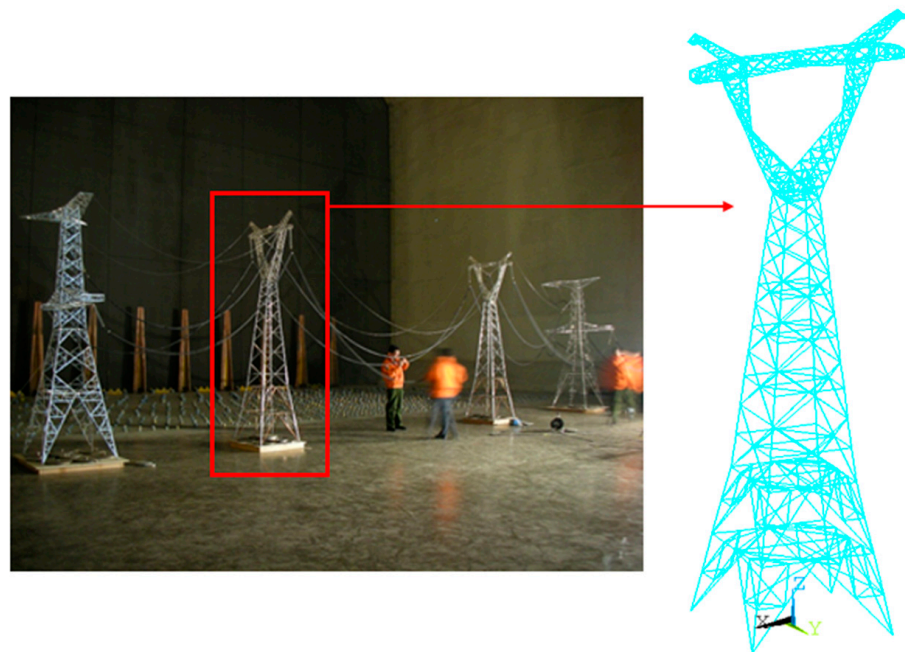


Figure 2. An in-service transmission tower model.

4.2. The Time-Varying Performance Function of the In-Service Transmission Tower

4.2.1. The Probabilistic Statistical Characteristics

The probabilistic statistical characteristics of the random parameters of this in-service transmission tower are listed in Table 1 [37]. In this paper, the design wind speed of reference height is considered as 30 m/s, and the load condition of 90 degrees wind condition is considered. Since the coupling between the transmission line and the transmission tower is quite complex, the self-weight and the wind loads of the transmission line are assigned to each hanging point of the transmission tower in this paper.

Table 1. Statistical characteristics of random parameters.

Variables	Physical Meaning	Probability Distribution	Mean	COV
E_s	Elastic modulus	Normal	206 GPa	0.03
ν	Poisson’s ratio	Normal	0.3	0.03
f_{y0-345}	Yield strength of Q345 steel	Normal	387.1 MPa	0.07
f_{y0-235}	Yield strength of Q235 steel	Normal	263.7 MPa	0.07

4.2.2. Random Equivalent Static Wind Loads

The design reference period $T = 50$ years is considered, and the transmission tower is divided into 36 sections along the height direction. By combining the calculation formula of standard value of the wind loads in DL/T 5154-2012 [23] and Equations (2a)–(4) in this paper, the mean and standard deviation of wind loads along the height of the tower can be obtained. Meanwhile, the calculation results are shown in Table 2, where the random equivalent static wind loads are considered as the type I extreme distribution.

Table 2. Statistical characteristics of random equivalent static wind loads.

No.	Height of Tower (m)	Mean (kN)	Standard Deviation (kN)	No.	Height of Tower (m)	Mean (kN)	Standard Deviation (kN)
1	12.00	18.49	3.57	19	143.96	19.20	3.71
2	24.00	48.70	9.40	20	148.27	19.39	3.74
3	34.50	29.05	5.61	21	147.58	19.36	3.74
4	45.00	71.35	13.77	22	152.00	35.25	6.80
5	64.00	84.35	16.28	23	155.20	15.81	3.05
6	80.60	85.32	16.47	24	158.40	15.90	3.07
7	95.10	79.03	15.25	25	161.60	15.99	3.09
8	106.60	62.21	12.01	26	164.80	16.09	3.11
9	115.10	49.43	9.54	27	168.00	16.18	3.12
10	122.70	47.59	9.18	28	168.00	5.62	1.08
11	129.50	43.48	8.39	29	170.40	5.64	1.09
12	133.12	18.74	3.62	30	171.13	5.65	1.09
13	135.00	18.82	3.63	31	171.87	5.66	1.09
14	138.32	18.96	3.66	32	172.60	5.67	1.09
15	136.73	18.89	3.65	33	174.93	5.69	1.10
16	141.63	19.10	3.69	34	177.27	5.71	1.10
17	140.35	19.05	3.68	35	179.60	5.74	1.11
18	144.95	19.25	3.71	36	181.80	5.76	1.11

4.2.3. Resistance Degradation Model of the In-Service Transmission

On the time-varying performance of the in-service transmission towers, the influence of the degradation of yield strength of steel members is considered in this paper, and the resistance $R(t)$ in Equation (1) is taken as yield strength $f_y(t)$ here. Therefore, according to the relationship between the $f_y(t)$ of corroded steel and the corrosion damage factor $w_s(t)$ suggested in Ref. [38], the Equation (1) can be rewritten as

$$f_y(t) = f_{y0}\xi(t) = f_{y0}(1 - 0.9852w_s(t)) \tag{22a}$$

$$w_s(t) = \begin{cases} L_0\alpha K(1 - p)t / A_0, t < t_L \\ L_0\alpha K[(1 - p)t_L + t - t_L] / A_0, t \geq t_L \end{cases} \tag{22b}$$

where f_{y0} is the initial yield strength of steel members, L_0 and A_0 denote the initial perimeter and initial area of steel members, respectively, t_L is the anti-corrosion life of different anti-corrosion strategies, and is taken as 10 years here, α is the distinguishing coefficient between ordinary steel and weathering steel with the value of 0.7, K is the average corrosion rate of steel members on one side with the value of 0.025 mm/year, and p is the protection efficiency and is taken as 95% here.

4.2.4. The Time-Varying Equivalent Performance Function

According to the resistance degradation model shown in Equations (22a) and (22b), the time-varying equivalent performance function of the in-service transmission tower can be obtained based on Equation (5a), namely

$$Z(t) = \min_{i=1,2,\dots,l} [f_y(t) - S_i(W_{seT}, t)] \tag{23}$$

where l represents the number of members, i.e., $l = 1053$.

4.3. The Time-Varying Global Reliability Analysis Based on the HM-IMEM of the In-Service Transmission Tower at $t = 30$

The time-varying reliability of the in-service transmission tower is investigated at intervals of 10 years, i.e., $\{t_0 = 0, t_1 = 10, t_2 = 20, t_3 = 30, t_4 = 40, \text{ and } t_5 = 50\}$. In order to

explain the implementation process of the proposed method, $t_3 = 30$ is taken as an example to illustrate in detail the implementation process by the proposed method.

4.3.1. The Estimation of the High-Order Moments Based on the GF-Discrepancy-Based Point Selection Method

Firstly, 200 sample points are selected by Equations (9)–(13b), shown in Figure 3, and the corresponding weight coefficients are obtained.

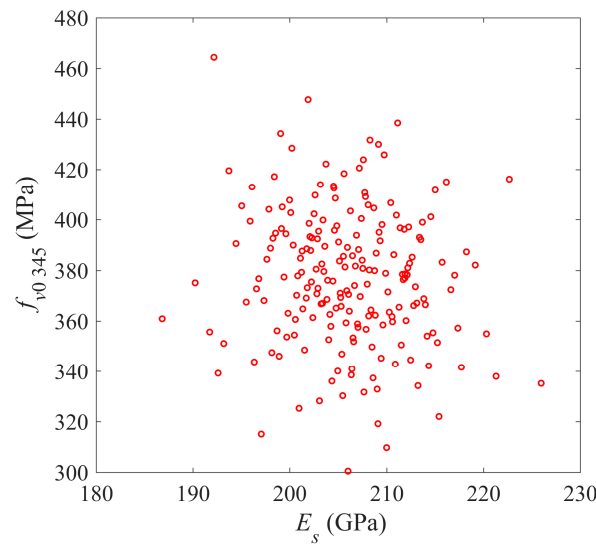


Figure 3. Sample point.

Then, the structural response values of each moment are obtained by structural reanalysis of 200 sample points. The raw moments of the structural response are calculated by Equation (14) and the results are shown in Table 3.

Table 3. The results of the raw moments.

Raw Moments	MCS	The Proposed Method	Relative Error ϵ (%)
$M_{Z,1}$	8.9690×10^7	8.9231×10^7	0.51
$M_{Z,2}$	8.7464×10^{15}	8.6250×10^{15}	1.39
$M_{Z,3}$	9.1014×10^{23}	8.8797×10^{23}	2.44
$M_{Z,4}$	9.9986×10^{31}	9.6338×10^{31}	3.65
$M_{Z,5}$	1.1512×10^{40}	1.0931×10^{40}	5.05
$M_{Z,6}$	1.3815×10^{48}	1.2897×10^{48}	6.64

4.3.2. The Determination of Integral Limits and Order of the High-Order Moments

Based on Equations (15) and (16c), the upper and lower integral limits of the HM-IMEM are -1.1423×10^8 and 2.9308×10^8 , respectively. Furthermore, based on Equation (17), the order of the high-order moments required by the HM-IMEM is determined to be 6.

4.3.3. The Structural Reliability Analysis

Finally, the reliability index of $t_r = 30$ is calculated based on Equations (18)–(21), and the calculation results are shown in Tables 4 and 5. In order to verify the accuracy of the proposed method, the reliability index calculated by the traditional MEM is given, and the MCS with 3×10^6 sample points is used as the standard solution.

Table 4. Evolution of the estimated reliability index and its Shannon entropy with the variation in s .

	$s = 2$	$s = 4$	$s = 6$
β	3.466	3.701	3.802
$\varepsilon(\%)$	8.74	2.55	0.11
H_s	18.4827	18.4822	18.4822

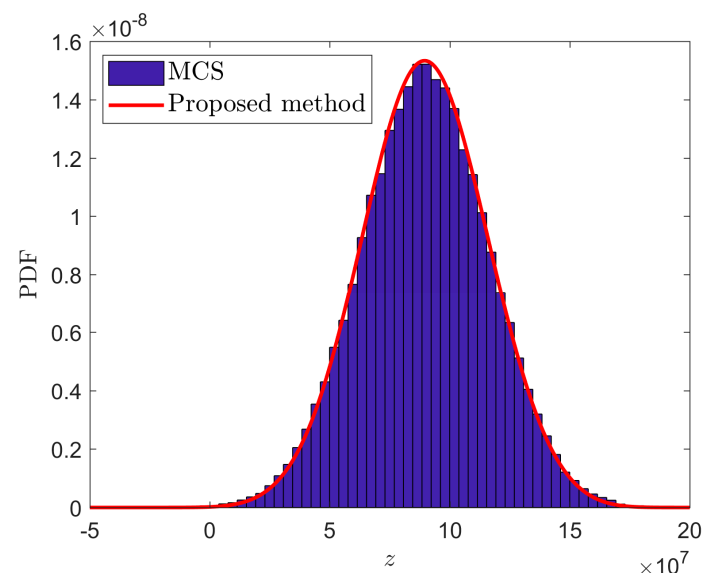
Table 5. Comparison of estimated reliability index for different approaches.

	MCS	Traditional MEM	The Proposed Method
β	3.798	3.390	3.802
$\varepsilon(\%)$	—	10.72	0.11

Table 5 shows that the reliability index of the proposed method is 3.802, which is almost identical to the reliability index of MCS, which is 3.798. This indicates that the proposed method can provide highly accurate reliability results, with a relative error of only 0.11%. In contrast, the traditional MEM based on the first four moments [24] could not yield accurate results, with a relative error of the reliability index as large as 10.72%. These results demonstrate that for global reliability analysis of in-service transmission towers, the proposed method significantly improves the accuracy of the traditional MEM.

4.3.4. Calculation of the Maximum Entropy PDF

In addition, the PDF obtained from the proposed method and MCS is also compared in Figure 4. It is easy to find that the results of the proposed method are in good agreement with those of MCS, indicating that the proposed method can accurately fit the PDF of the performance function of the in-service transmission tower in the entire range of probability distribution. In terms of computational efficiency, the proposed method requires much fewer structural analyses than MCS, which shows that the proposed method is more efficient.

**Figure 4.** PDF curve of the proposed method and MCS method at $t = 30$.

4.4. The Time-Varying Global Reliability Analysis Results during the Design Reference Period

Similarly, by following the above process, the reliability index and the corresponding PDF of t_r ($r = 0, 10, 20, \dots, 50$) can be calculated, respectively, as shown in Figures 5 and 6. Figure 5 indicates that after 50 years of service, the reliability index of the transmission tower decreases from 4.32 to 3.39, with a decrease of 0.93, which shows a significant reduction

in the reliability index of the in-service transmission tower. Therefore, it is necessary to analyze the time-varying reliability of the in-service transmission tower. Moreover, the reliability index decreases faster nearly 10 years later, because the corrosion life t_L of the in-service transmission tower is taken as 10 years, which also indicates that the in-service transmission tower exceeding the corrosion life must be treated with corrosion protection to slow down the degradation process. Figure 6 shows that the PDF gradually shifts to the left over time, which denotes an increase in the failure domain, and the change in failure probability is consistent with the gradual decrease in the reliability index of the in-service transmission tower over time.

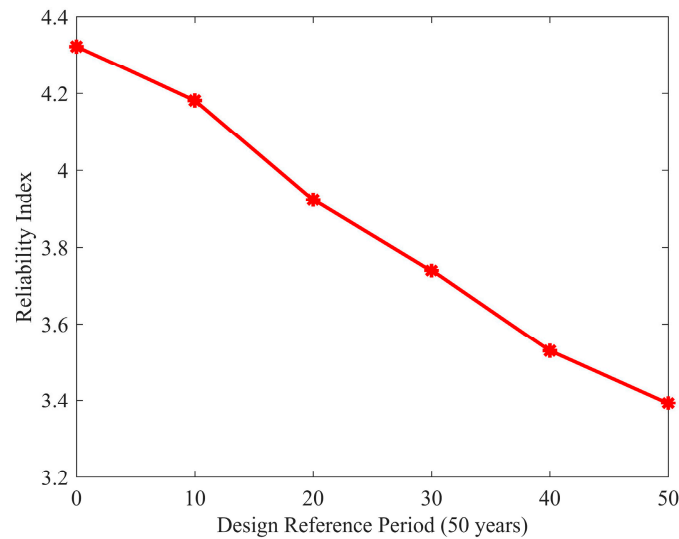


Figure 5. Time-varying reliability index of the in-service transmission tower.

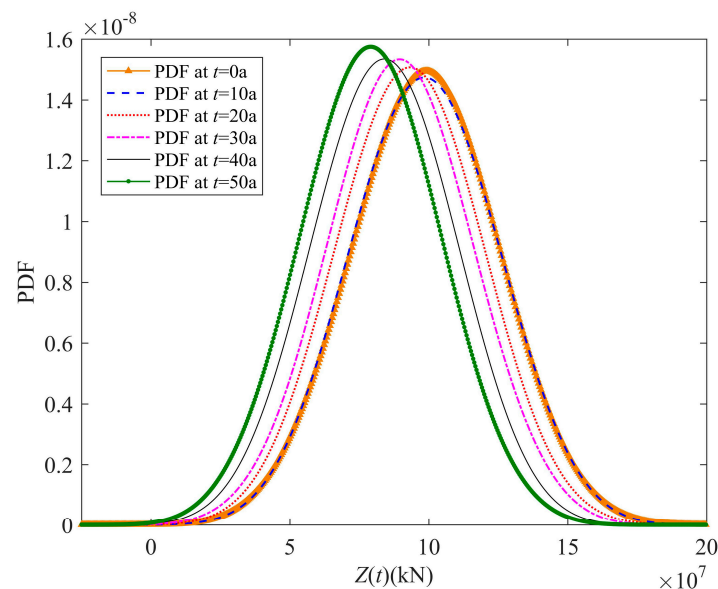


Figure 6. PDF for different t_r .

5. Conclusions

In this paper, a time-varying global reliability analysis method for in-service transmission towers based on the HM-IMEM is proposed and verified by an actual engineering example. The main conclusions can be drawn as follows:

- (1) The time-varying equivalent performance function of the in-service transmission tower is established based on the resistance degradation model of steel members and the random equivalent static wind loads;
- (2) A high-order moments-based improved maximum entropy method for time-varying global reliability analysis of the in-service transmission tower is developed;
- (3) The MCS is used to calculate the reliability index at a typical time as the standard solution. The relative error of the reliability results of the proposed method is just 0.11%, which demonstrates that the proposed method can provide fairly high accuracy for reliability results;
- (4) The proposed method has high computational efficiency and much lower computational cost than MCS;
- (5) The reliability index of the in-service transmission tower is significantly reduced after a certain period of time, and it is necessary to analyze the time-varying reliability of the in-service transmission tower to evaluate its safety status.

Author Contributions: Conceptualization, C.L. and T.W.; Methodology, C.L. and T.W.; Software, Z.T.; Data curation, Z.T.; Writing—Original draft preparation, C.L.; Writing—Review and editing, C.L. and T.W.; Supervision, T.W.; Project administration, Z.L.; Funding acquisition, Z.L. All authors have read and agreed to the published version of the manuscript.

Funding: This research was funded by [NSFC-JSPS China-Japan Scientific Cooperation Project] grant number [No. 51611140123], and was funded by [Special Postdoctoral Support Project of Chongqing Research Institute of HIT (Life-cycle reliability assessment of the power transmission tower in the mountainous area under the wind-ice disaster)].

Institutional Review Board Statement: Not applicable.

Informed Consent Statement: Not applicable.

Data Availability Statement: The data used to support the findings of this study are included in the article.

Conflicts of Interest: The authors declare that they have no known competing financial interests or personal relationships that could have appeared to influence the work reported in this paper.

References

1. Albermani, F.; Kitipornchai, S.; Chan, R.W.K. Failure analysis of transmission towers. *Eng. Fail. Anal.* **2009**, *16*, 1922–1928. [[CrossRef](#)]
2. Rao, N.P.; Knight, G.M.S.; Lakshmanan, N.; Iyer, N.R. Investigation of transmission line tower failures. *Eng. Fail. Anal.* **2010**, *17*, 1127–1141.
3. Tang, Z.Q.; Li, Z.L.; Wang, T. Probabilistic bearing capacity assessment for unequal-leg angle cross-bracings in transmission towers. *J. Constr. Steel. Res.* **2023**, *200*, 107672. [[CrossRef](#)]
4. Liu, Z.H.; Liu, Z.Z.; He, C.G.; Lu, H.L. Dimension-reduced probabilistic approach of 3-D wind field for wind-induced response analysis of transmission tower. *J. Wind. Eng. Ind. Aerod.* **2019**, *190*, 309–321. [[CrossRef](#)]
5. Mangalathu, S.; Jang, H.; Hwang, S.; Jeon, J. Data-driven machine-learning-based seismic failure mode identification of reinforced concrete shear walls. *Eng. Struct.* **2020**, *208*, 110331. [[CrossRef](#)]
6. Deng, H.Z.; Wang, Z.M. A study for the limit strength and reliability of transmission tower structural system. *Electric. Power Constr.* **2000**, *21*, 12–14.
7. Li, M.; Li, Z.; Ren, J. Reliability analysis on tower structure for 500 kV transmission lines. *Power Syst. Technol.* **2008**, *32*, 91–95.
8. Wang, T.; Li, Z.L.; Fan, W.L.; Ang, A.H.S. Structural system reliability assessment using generalized factorized dimensional reduction method and iterative maximum entropy method. *Struct. Infrastruct. Eng.* **2022**, 1–12. [[CrossRef](#)]
9. Yu, D.K.; Li, Z.L.; Li, M.H.; Fan, W.L. Wind-resistant reliability analysis of UHV transmission tower based on moment methods. *Eng. Mech.* **2013**, *30*, 311–316.
10. Gong, J.X.; Zhao, G.F. Reliability analysis for deteriorating structures. *J. Build. Struct.* **1998**, *19*, 43–51.
11. Tvedt, L. Vector Process Out-Crossing as Parallel System Sensitivity Measure. *J. Eng. Mech.* **1991**, *121*, 2201–2210.
12. Sudret, B. Analytical derivation of the outcrossing rate in time-variant reliability problems. *Struct. Infrastruct. Eng.* **2008**, *4*, 353–362. [[CrossRef](#)]
13. Zhang, J.F.; Du, X.P. Time-dependent reliability analysis for function generation mechanisms with random joint clearances. *Mech. Mach. Theory* **2015**, *92*, 184–199. [[CrossRef](#)]

14. Li, X.L.; Chen, G.H.; Wang, Y.T.; Yang, D.X. A unified approach for time-invariant and time-variant reliability-based design optimization with multiple most probable points. *Mech. Syst. Signal Process.* **2022**, *177*, 109176. [[CrossRef](#)]
15. Li, J.; Chen, J.B. The probability density evolution method for dynamic response analysis of non-linear stochastic structures. *Int. J. Numer. Methods Eng.* **2006**, *65*, 882–903. [[CrossRef](#)]
16. Mori, Y.; Ellingwood, B.R. Time-dependent system reliability analysis by adaptive importance sampling. *Struct. Saf.* **1993**, *12*, 59–73. [[CrossRef](#)]
17. Zhou, Q.Y.; Li, Z.L.; Fan, W.L.; Ang, A.H.-S.; Liu, R. System reliability assessment of deteriorating structures subjected to time-invariant loads based on improved moment method. *Struct. Saf.* **2017**, *68*, 54–64. [[CrossRef](#)]
18. Gong, J.X.; Zhao, G.F. Fatigue reliability analysis for corroded reinforced concrete structures corroded reinforced concrete structures. *China Civ. Eng. J.* **2000**, *33*, 50–56.
19. Heo, W.H. Performance-based reliability estimates for highway bridges considering previous inspection data. *Appl. Sci.* **2020**, *10*, 1873. [[CrossRef](#)]
20. Brignone, M.; Mestriner, D.; Procopio, R.; Delfino, F. A review on the return stroke engineering models attenuation function: Proposed expressions, validation and identification methods. *Electr. Power Syst. Res.* **2019**, *172*, 230–241. [[CrossRef](#)]
21. Cooray, V.; Rubinstein, M.; Rachidi, F. Modified transmission line model with a current attenuation function derived from the lightning radiation field—MTLD model. *Atmosphere* **2021**, *12*, 249. [[CrossRef](#)]
22. Li, J.; Chen, J.B.; Fan, W.L. The equivalent extreme-value event and evaluation of the structural system reliability. *Struct. Saf.* **2007**, *29*, 112–131. [[CrossRef](#)]
23. DL/T 5486-2020; National Energy Administration, Technical Specification for the Design of Steel Supporting Structures of Overhead Transmission Line. China Planning Press: Beijing, China, 2020.
24. Li, G.; Zhang, K. A combined reliability analysis approach with dimension reduction method and maximum entropy method. *Struct. Multidiscip. Optim.* **2011**, *43*, 121–134. [[CrossRef](#)]
25. Lv, Y.B.; Hu, T.S.; Wang, G.M.; Wan, Z.P. A penalty function method based on Kuhn–Tucker condition for solving linear bilevel programming. *Appl. Math. Comput.* **2007**, *188*, 808–813. [[CrossRef](#)]
26. Antczak, T. Exact penalty functions method for mathematical programming problems involving invex functions. *Eur. J. Oper. Res.* **2009**, *198*, 29–36. [[CrossRef](#)]
27. Dehghani, R.; Hosseini, M.M.; Bidabadi, N. The modified quasi-newton methods for solving unconstrained optimization problems. *Int. J. Numer. Model.* **2019**, *32*, e2459. [[CrossRef](#)]
28. Wei, Z.; Li, G.; Qi, L. New quasi-newton methods for unconstrained optimization problems. *Appl. Math. Comput.* **2006**, *175*, 1156–1188. [[CrossRef](#)]
29. Wan, Z.; Teo, K.L.; Shen, X.; Hu, C. New BFGS method for unconstrained optimization problem based on modified armijo line search. *Optimization* **2014**, *63*, 285–304. [[CrossRef](#)]
30. Zhang, Z.; Jiang, C.; Han, X.; Ruan, X.X. A high-precision probabilistic uncertainty propagation method for problems involving multimodal distributions. *Mech. Syst. Signal Process.* **2019**, *126*, 21–41. [[CrossRef](#)]
31. Rajan, A.; Kuang, Y.C.; Ooi, M.P.L.; Demidenko, S.N.; Carstens, H. Moment-constrained maximum entropy method for expanded uncertainty evaluation. *IEEE Access* **2018**, *6*, 4072–4082. [[CrossRef](#)]
32. Chen, J.B.; Yang, J.; Li, J. A GF-discrepancy for point selection in stochastic seismic response analysis of structures with uncertain parameters. *Struct. Saf.* **2016**, *59*, 20–31. [[CrossRef](#)]
33. Chen, J.B.; Ghanem, R.; Li, J. Partition of the probability-assigned space in probability density evolution analysis of nonlinear stochastic structures. *Probabilistic Eng. Mech.* **2009**, *24*, 27–42. [[CrossRef](#)]
34. Joe, S.; Kuo, F.Y. Constructing Sobol sequences with better two-dimensional projections. *SIAM. J. Sci. Comput.* **2008**, *30*, 2635–2654. [[CrossRef](#)]
35. Racz, S.; Tari, A.; Telek, M. A moments based distribution bounding method. *Math. Comput. Model.* **2006**, *43*, 1367–1382. [[CrossRef](#)]
36. Li, Z.L.; Xiao, Z.Z.; Han, F.; Yan, Z.T. Aeroelastic model design and wind tunnel tests of 1000 kV Hanjiang long span transmission line system. *Power Syst. Technol.* **2008**, *32*, 1–5.
37. Joint Committee on Structural Safety. JCSS—2001 Probabilistic Model Code-Part 3-Resistance Models; Joint Committee on Structural Safety: Copenhagen, Denmark, 2001.
38. Shi, W.Z.; Tong, L.W.; Chen, Y.Y.; Li, Z.; Shen, K. Experimental study on influence of corrosion on behavior of steel material and steel beams. *J. Build. Struct.* **2012**, *33*, 53–60.

Disclaimer/Publisher’s Note: The statements, opinions and data contained in all publications are solely those of the individual author(s) and contributor(s) and not of MDPI and/or the editor(s). MDPI and/or the editor(s) disclaim responsibility for any injury to people or property resulting from any ideas, methods, instructions or products referred to in the content.